Research Article

Tian Su, Ting Wang, Zhaochuan Zhang, Xiao Sun, Shangwei Gong, Xuefeng Mei, Zhenyu Tan, and Shenao Cui*

Mechanical properties and frost resistance of recycled brick aggregate concrete modified by nano-SiO_2

https://doi.org/10.1515/ntrev-2023-0576
received March 29, 2023; accepted June 30, 2023

Abstract: In this work, brick aggregates were immersed in nano-SiO_2 solution for 2 days, and the effects of nano-SiO_2 on the brick aggregate properties, mechanical properties (compressive strength, flexural strength, and splitting tensile strength), frost resistance (apparent phenomenon, mass loss, relative dynamic modulus of elasticity, and compressive strength) of recycled brick aggregate concrete and the microstructure of recycled brick aggregate concrete were investigated. The results show that nano-SiO_2 can effectively improve the performance of recycled brick aggregate and the mechanical properties of recycled brick aggregate concrete, mainly by reducing the water absorption and crushing index and improving the compressive strength, flexural strength, and splitting tensile strength. With increasing nano-SiO_2 solution concentration, the compressive strength, flexural strength, and splitting tensile strength of recycled brick aggregate concrete first increase and then decrease. The frost resistance of recycled brick aggregate concrete is superior to that of ordinary aggregate concrete, while the frost resistance of nano-SiO_2-modified recycled brick aggregate concrete is inferior to that of recycled brick aggregate concrete. In addition, the freeze–thaw damage mechanism of recycled brick aggregate concrete is analyzed, and a freeze–thaw damage life prediction model of nano-SiO_2-modified recycled brick aggregate concrete based on the Weibull distribution is proposed.

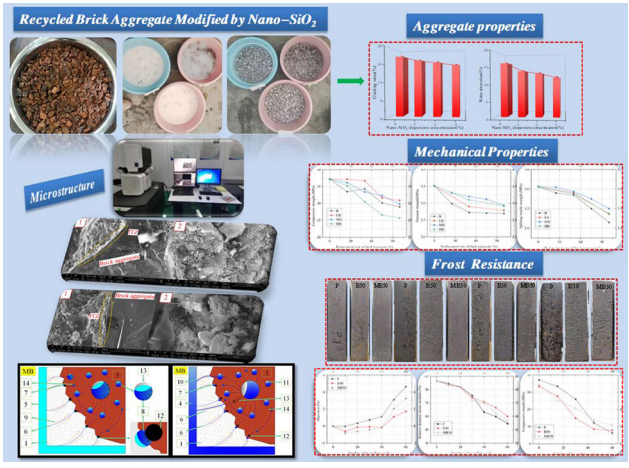

Graphical abstract

Keywords: recycled brick aggregate, nano-SiO_2, mechanical property, frost resistance, microstructure, life prediction model

1 Introduction

With the increasing demand for infrastructure construction in various countries, a large amount of natural resources are consumed. At the same time, a large number of construction waste materials and construction waste are generated during the construction and demolition process, causing serious environmental pollution problems [1]. The composition of construction waste is complex, among which waste concrete and waste bricks account for a large proportion. According to statistics provided by the United States Environmental Protection Agency, from 2012 to 2014, approximately 44 million tons of waste bricks were generated from construction and

* **Corresponding author: Shenao Cui,** School of Civil and Architectural Engineering, Shandong University of Technology, Zibo, 255000, China, e-mail: cuishenao0523@outlook.com
Tian Su: School of Civil and Architectural Engineering, Shandong University of Technology, Zibo, 255000, China; School of Civil Engineering, Wuhan University, 8 Donghu South Road, Wuhan, Hubei, 430072, China; China Railway 11 Bureau Group Co., Ltd, 277 Zhongshan Road, Wuhan, Hubei, 430061, China; International College, Krirk University, No. 3 Soi Ramintra 1, Ramintra Road, Anusaowaree, Bang Khen, Bangkok 10220, Thailand
Ting Wang, Zhaochuan Zhang, Xiao Sun, Shangwei Gong, Xuefeng Mei: School of Civil and Architectural Engineering, Shandong University of Technology, Zibo, 255000, China
Zhenyu Tan: International College, Krirk University, No. 3 Soi Ramintra 1, Ramintra Road, Anusaowaree, Bang Khen, Bangkok 10220, Thailand

Open Access. © 2023 the author(s), published by De Gruyter. This work is licensed under the Creative Commons Attribution 4.0 International License.

demolition activities [2]. In China, there are approximately 400 million tons of waste bricks every year [3]. To realize the resource utilization of construction waste, the technology of recycled aggregate concrete has been proposed and has been widely studied by scholars all over the world.

Due to the mortar attached to the surface of the recycled coarse aggregate, the porosity and water absorption of the aggregate were high [4]. The concrete prepared by recycled coarse aggregate had multiple interface transition zones and a large number of microcracks and pores in the interface transition zone, resulting in the mechanical properties and frost resistance of recycled coarse aggregate concrete being generally inferior to ordinary concrete [5]. Compared with recycled stone aggregate, recycled brick aggregate had more pores and cracks, small hardness, high water absorption, and large crushing index, resulting in two weak links of recycled brick aggregate concrete: interface transition zone and recycled brick aggregate [6]. The replacement of natural aggregate with recycled stone aggregate and recycled brick aggregate reduced the mechanical properties of concrete, and with the increase in the replacement rate of recycled aggregate, the mechanical properties of concrete decreased.

Freeze–thaw damage is an important threat to reinforced concrete buildings in cold regions [7]. Freeze–thaw damage leads to concrete frost heaving and cracking [8], which causes corrosion of internal reinforcement and seriously threatens the long-term safe use of concrete structures [9,10]. The frost resistance of concrete is affected by many factors, such as porosity, pore structure, water-cement ratio, environmental conditions, and aggregate type [11]. Due to the adhesion of old cement mortar on the surface of recycled aggregate and the secondary damage during the crushing process [12], the porosity of aggregate was increased, the pore structure deteriorated [13], and the type of aggregate was changed [14], resulting in the frost resistance of recycled aggregate concrete being inferior to that of ordinary concrete [15]. When the number of freeze–thaw cycles was small, the frost resistance of recycled concrete was not significantly different from that of ordinary concrete; with the increase in the number of freeze–thaw cycles, the frost resistance of recycled concrete deteriorated more seriously [16]. With the increasing number of freeze–thaw cycles, the mass loss rate, relative dynamic modulus loss, and compressive strength loss of recycled concrete were significantly faster [17]. In addition, with the increase in the replacement rate of recycled aggregate, this phenomenon was more significant [18]. In particular, concrete containing recycled brick aggregate had worse frost resistance than recycled stone concrete [19], and its frost resistance must be improved to achieve its application in cold regions [20]. Therefore, improving the frost resistance of recycled concrete has become a research hotspot.

Domestic and foreign scholars have carried out corresponding research on improving the frost resistance of recycled concrete and have achieved some results [21]. The frost resistance of recycled concrete could be enhanced by reducing the water-cement ratio of concrete [22], improving the aggregate distribution and quality [23], adding silica fume or air-entraining agent [24], and using the aggregate produced by the original concrete with air-entraining agent [25,26].

In recent years, nanomaterials have been gradually applied to improve the mechanical properties and frost resistance of recycled concrete [27,28]. Among nanomaterials, nano-SiO_2 not only has the advantages of high permeability [29], high specific surface energy, and good hydrophilicity but can also accelerate the hydration rate of cement [30] and improve the mechanical properties and porosity of concrete [31]. Therefore, nano-SiO_2 began to be applied to enhance the performance of recycled concrete. Shahbazpanahi *et al.* [32] found that the incorporation of nano-SiO_2 made the interfacial transition zone between recycled aggregate and mortar denser, increasing the C–S–H content, reducing the content of CH and AFt, and improving the internal pore structure of concrete. Li *et al.* [33] noted that nano-SiO_2 could significantly enhance the microhardness of the interface transition zone, thereby improving the mechanical properties and durability of concrete [34,35]. However, the incorporation of nano-SiO_2 should be controlled within a certain range. If the incorporation of nano-SiO_2 was too large, it could lead to a decrease in the mechanical properties and durability of concrete [36,37].

The poor performance of recycled aggregate was the main reason for the poor mechanical properties and durability of recycled concrete [38,39]. Therefore, improving the performance of recycled aggregate could effectively improve the mechanical properties and durability of recycled concrete [40]. Meng *et al.* [41] found that after the modification of nanomaterials, the crushing index of recycled coarse aggregate decreased, which improved the mechanical properties of recycled concrete. Wang *et al.* [42] noted that after the modification of nanomaterials, the water absorption and crushing index of recycled brick aggregate decreased, while the compressive strength of brick aggregate concrete at different ages increased.

In the existing research, there have been relatively few studies on the frost resistance of concrete prepared by nano-modified recycled aggregate. However, improving the frost resistance of recycled concrete is the key to its application in cold regions. The objective of this study is to investigate the mechanical properties and frost resistance of recycled brick aggregate concrete modified by nano-SiO_2 and compare them with those of unmodified brick

aggregate concrete and ordinary concrete, investigate the effects of nano-SiO_2 on the microstructure of recycled brick aggregate concrete, and propose a freeze–thaw damage life prediction model of nano-modified recycled brick aggregate concrete based on the Weibull distribution.

2 Experimental overview

2.1 Raw materials

1) Cement

P.O 42.5 ordinary Portland cement used for the concrete mixtures was produced by Zibo Shanshui Cement Co., Ltd. The physical performance and chemical composition are listed in Tables 1 and 2, respectively.

2) Fine aggregate

Natural river sand was used as fine aggregate conforming to the Chinese standard GB/T 14684–2011 [43], and the fineness modulus was 2.9.

3) Coarse aggregate

Coarse aggregates included natural gravel and recycled brick aggregates with a particle size of 5–25 mm. The water absorption of natural aggregate and recycled brick aggregate was 1.10 and 16.50%, respectively, and the crushing index was 8.70 and 27.90%, respectively.

4) Nanomaterial

Nano-SiO_2 with a particle size of 20 nm was selected, and the properties are listed in Table 3.

2.2 Recycled brick aggregate modified by nanomaterials

The recycled bricks were crushed by a jaw crusher, and then the recycled brick aggregates were cleaned and dried. Finally, the recycled brick aggregates were graded to meet the requirements of aggregate distribution.

Nano-SiO_2 powder was added to the solution and mechanically stirred for 5 min. The brick aggregate was immersed in 1, 2, and 3% nano-SiO_2 solutions for 2 days, and the nano-SiO_2 solution was dispersed by an ultrasonic disperser to prevent particle agglomeration. The process is shown in Figure 1.

Table 2: Chemical composition of P.O 42.5 ordinary Portland cement

Chemical composition	SiO_2	Al_2O_3	Fe_2O_3	CaO	MgO	SO_3
Content (%)	21.6	5.78	3.96	61.25	1.76	2.46

Table 3: Properties of nano-SiO_2

Particle size (nm)	Specific surface area ($m^2\ g^{-1}$)	Bulk density ($g\ m^{-3}$)
20	240	0.06

2.3 Mixture proportion

The mixture proportions of natural aggregate concrete and recycled brick aggregate concrete were designed according to JGJ55-2011 [44], and the design water-to-binder (w/b) ratio of concrete was 0.5, as detailed in Table 4 (due to the large difference between the density of recycled brick aggregate and natural aggregate, this study adopted the volume substitution method to ensure that the absolute volume of each cubic meter of concrete remained unchanged). It should be noted that the recycled brick aggregate was soaked with nano-SiO_2 solution at concentrations of 0, 1, 2, and 3% before being used.

2.4 Test method

2.4.1 Mechanical properties test

The mechanical properties of the concrete specimens were tested in accordance with GBT 50081–2019 [45], as shown in Figure 2, and the test details are shown in Table 5.

Table 1: Properties of P.O 42.5 ordinary Portland cement

Specific surface area ($m^2\ kg^{-1}$)	Ignition loss (%)	Initial/final setting times (min)	3 days/28 days flexural strength (MPa)	3 days/28 days compressive strength (MPa)
322	2.4	205/255	5.6/8.9	25.5/47.6

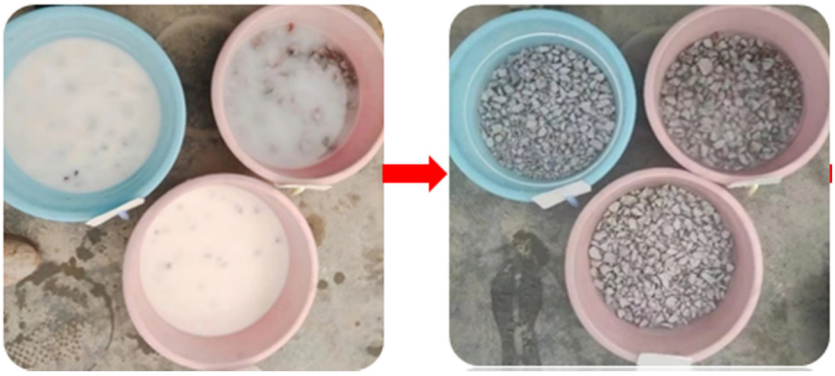

Figure 1: Aggregate modification process.

Table 4: Mix proportions of concrete (kg m^{-3})

Type	Water	Cement	Sand	NCA	RCA	*Q1**	*Q2**	*Q3**
p	175	350	700	1,140	0	0	0	0
B25	175	350	700	855	234	–	–	–
B50	175	350	700	570	468	–	–	–
B75	175	350	700	285	702	–	–	–
B100	175	350	700	0	936	–	–	–
LB25	175	350	700	855	–	234	–	–
LB50	175	350	700	570	–	468	–	–
LB75	175	350	700	285	–	702	–	–
LB100	175	350	700	0	–	936	–	–
MB25	175	350	700	855	–	–	234	–
MB50	175	350	700	570	–	–	468	–
MB75	175	350	700	285	–	–	702	–
MB100	175	350	700	0	–	–	936	–
HB25	175	350	700	855	–	–	–	234
HB50	175	350	700	570	–	–	–	468
HB75	175	350	700	285	–	–	–	702
HB100	175	350	700	0	–	–	–	936

*$Q1$, $Q2$, and $Q3$ are recycled brick aggregates modified with nano-SiO_2 solutions at concentrations of 1, 2, and 3%, respectively. The unmodified recycled brick aggregate was soaked in water for 2 days to ensure that it reached a saturated surface dry state.

2.4.2 Freeze–thaw cycle test

According to the Standard for Long-term Performance and Durability of Ordinary Concrete [46], the concrete prism specimens (100 mm × 100 mm × 400 mm) and concrete cube specimens (100 mm × 100 mm × 100 mm) were tested by a rapid freeze–thaw cycle testing machine, as shown in Figure 3.

2.4.3 Relative dynamic modulus elasticity test

The DT-10 W dynamic elastic modulus tester produced by Tianjin Luda Construction Instrument Co., Ltd was used to test concrete prism specimens under different freeze–thaw cycles, as shown in Figure 4.

2.4.4 Microstructure test

Microstructure tests include general microscope tests and electron microscope scanning tests. An electronic microscope produced by Jiangsu Leyes Technology Co., Ltd was used for the general microscope test, and field emission environmental scanning electron microscopy was used for the electron microscope scanning test, as shown in Figure 5.

Concrete specimens with a size of 15 mm × 15 mm × 15 mm were selected for observation under a general electronic microscope; concrete specimens with a size of 10 mm × 10 mm × 10 mm were selected for gold spraying treatment and then tested under a scanning electron microscope.

3 Results and analysis

3.1 Nano-modified recycled brick aggregate properties

The apparent phenomena of aggregates were observed through a general microscope, as shown in Figure 6. The surface of the stone aggregate was smooth with fewer pores and cracks, and its compactness was relatively high; the surface of the brick aggregate was rough with a large number of cracks and pores, and its compactness was low. After the brick aggregate is modified with nano-SiO_2, its surface pores and cracks are filled with nano-SiO_2 particles. As the concentration of nano-SiO_2 solution increased, the number and size of surface cracks and pores on the brick aggregate

Figure 2: Mechanical properties test. (a) Compressive strength test, (b) splitting tensile strength test, and (c) flexural strength test.

Table 5: Mechanical properties test details

Test	Specimen size (mm)	Conversion coefficient	Loading speed (MPa/s)
Compressive strength test	100 × 100 × 100	0.95	0.6
Flexural strength test	100 × 100 × 400	0.85	0.05
Splitting tensile strength test	100 × 100 × 100	0.85	0.05

gradually decreased, and the roughness gradually decreased. However, with the continuous increase in the concentration of the nano-SiO_2 solution, some nano-SiO_2 exhibited agglomeration phenomena. The reason for this phenomenon is that nano-SiO_2 is insoluble in water. When the concentration of nano-SiO_2 is too high, a small portion of nano-SiO_2 will enter the brick aggregate together with water, while another portion of nano-SiO_2 will adsorb on the surface of the brick aggregate due to its rough surface and even distribution. Most of the nano-SiO_2 will gradually settle on the surface of the brick aggregate under the action of gravity, which easily causes nano-SiO_2 agglomeration.

The crushing index and water absorption of recycled brick aggregate before and after nano-SiO_2 modification are shown in Figure 7. After nano-modification, the water absorption and crushing index of the recycled brick aggregate decreased, and with the increase in the nano-SiO_2 concentration, the water absorption and crushing index decreased more

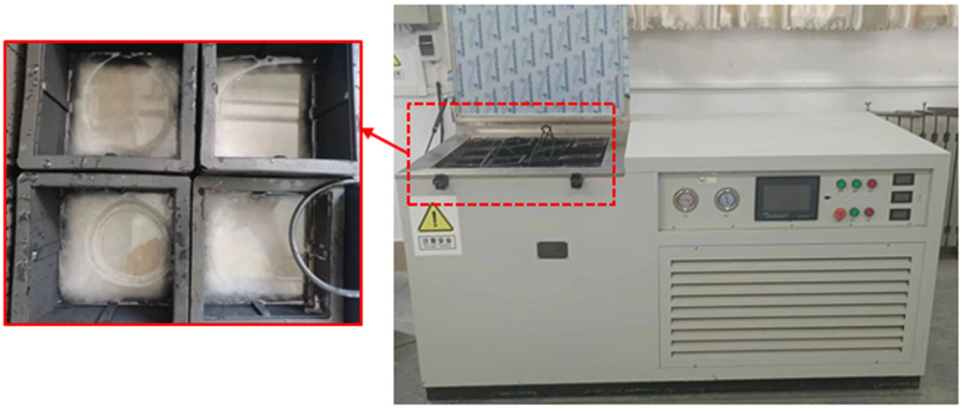

Figure 3: Rapid freeze–thaw cycle testing machine.

Figure 4: Relative dynamic modulus elasticity test.

significantly. The decrease in water absorption was larger than that of the crushing index, and the water absorption of recycled brick aggregate decreased by 15.09, 19.52, and 27.09%, respectively, after being modified by soaking in 1, 2, and 3% nano-SiO_2 solution, while the crushing index decreased by 6.74, 10.18, and 14.52%, respectively. This is due to the filling of recycled brick aggregate pores with nano-SiO_2, which reduces the water absorption and crushing index of the aggregate. This was consistent with the results of Wang *et al.* [42]. However, nano-SiO_2 does not react with the recycled brick aggregate and only fills the pores, with limited improvement in aggregate strength.

3.2 Mechanical properties

The compressive strength, flexural strength, and splitting tensile strength before and after nano-SiO_2 modification are shown in Figures 8–10. As the replacement rate of brick aggregate increased, the compressive strength, flexural strength, and splitting tensile strength of the concrete showed a downward trend, and the downward trend was increasingly obvious. The reasons are as follows: on the one hand, the recycled brick aggregate has low strength and high porosity, resulting in lower strength of concrete; while on the other hand, due to the high moisture content of the brick aggregate, the effective water cement ratio of concrete increases, which leads to a decrease in concrete strength.

After nano-SiO_2 modification, the compressive strength, flexural strength, and splitting tensile strength of recycled brick aggregate concrete were significantly improved. The reason is that nano-SiO_2 can fill the pores of recycled brick aggregate and increase the compactness of concrete. In addition, nano-SiO_2 has chemical activity, which can promote cement hydration and secondary reaction with $Ca(OH)_2$ to produce C–S–H gel to strengthen the interfacial transition zone between cement mortar and recycled brick aggregate, thereby improving the mechanical properties of recycled brick aggregate concrete.

With the increase in the nano-SiO_2 solution concentration, the compressive strength, flexural strength, and splitting tensile strength of recycled brick aggregate concrete first increased and then decreased. Therefore, when the concentration of nano-solution was 2%, the mechanical properties of recycled brick aggregate concrete were the best. This may be because although nano-SiO_2 is adsorbed on the recycled brick aggregate, it easily falls off and integrates into the cement mortar. With the increase in the nano-SiO_2 solution concentration, more nanomaterials are integrated into the cement mortar, and nano-SiO_2 is not easy to disperse in the wet state, which leads to the agglomeration of nano-SiO_2 and reduces the strength of concrete cement stone, thus reducing the strength of concrete.

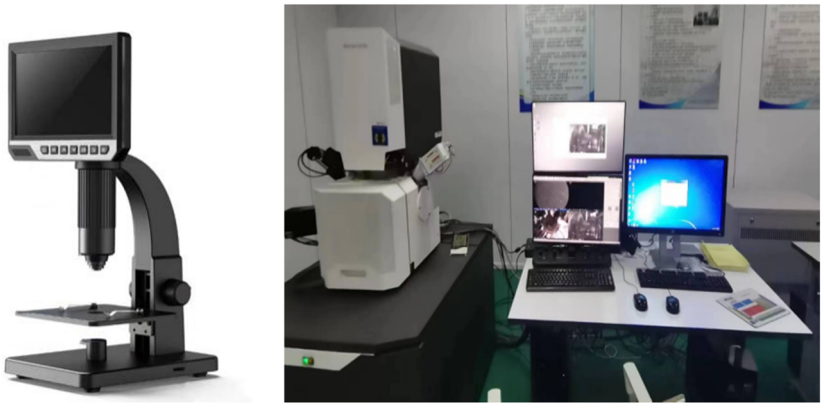

(a) (b)

Figure 5: Microstructure test. (a) General microscope test and (b) scanning electron microscope test.

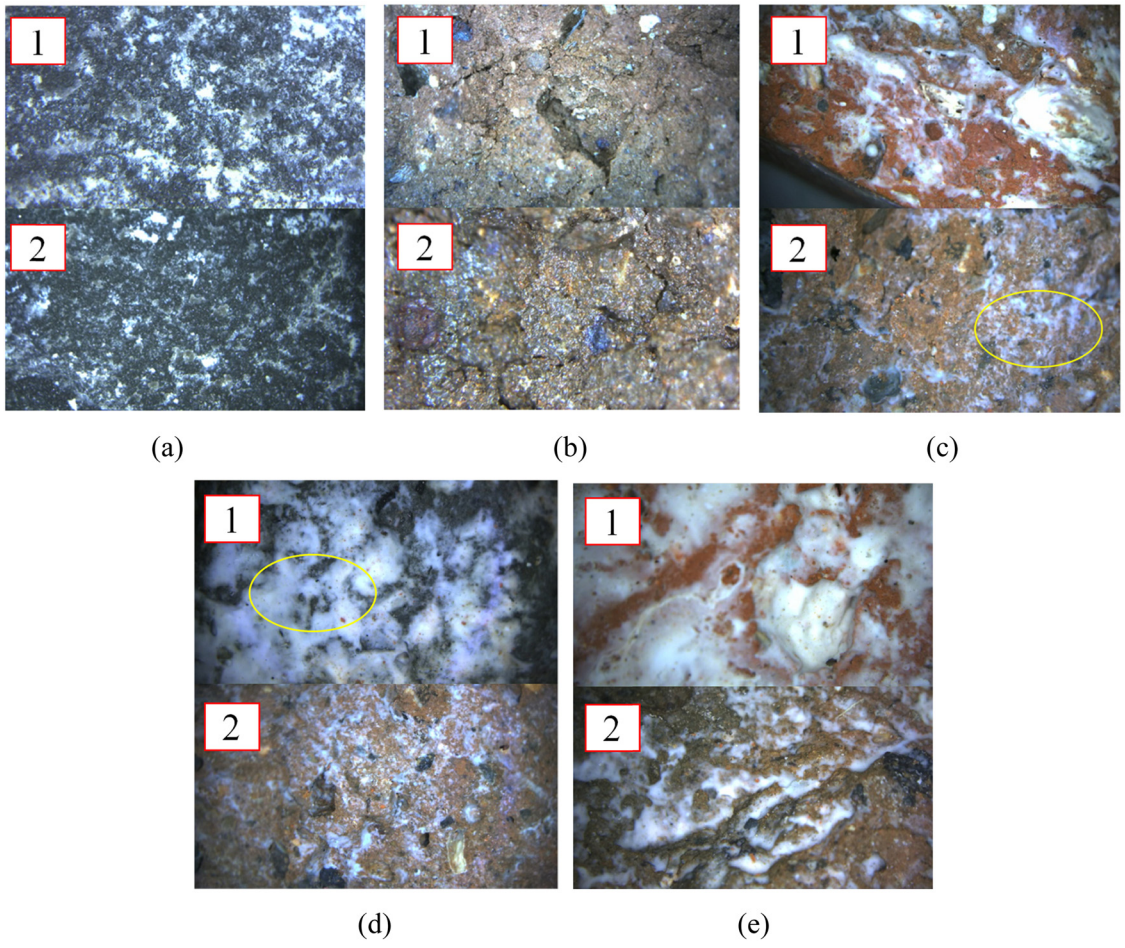

Figure 6: Apparent phenomena of aggregates before and after nano-SiO_2 modification. (a) P, (b) B, (c) LB, (d) MB, and (e) HB.

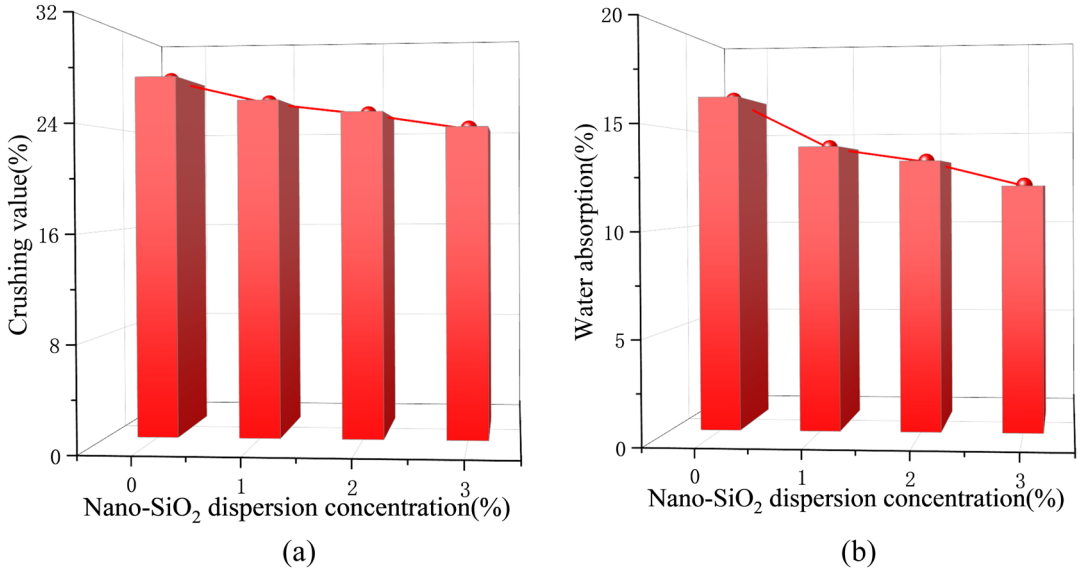

Figure 7: Aggregate properties before and after nano-SiO_2 modification. (a) Crushing index and (b) water absorption.

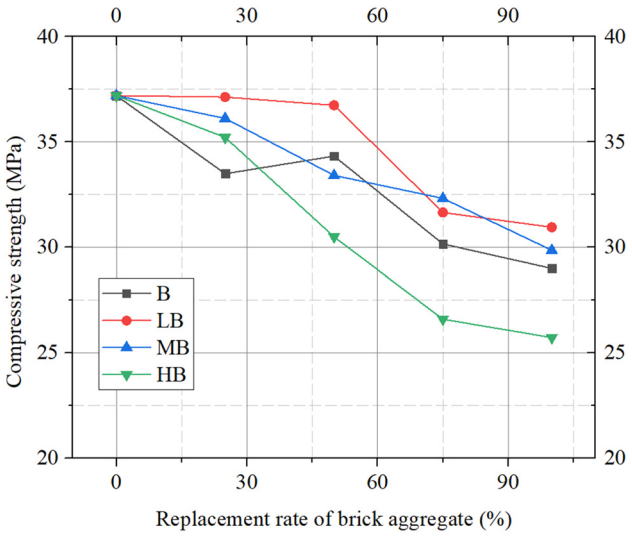

Figure 8: Compressive strength before and after nano-SiO_2 modification.

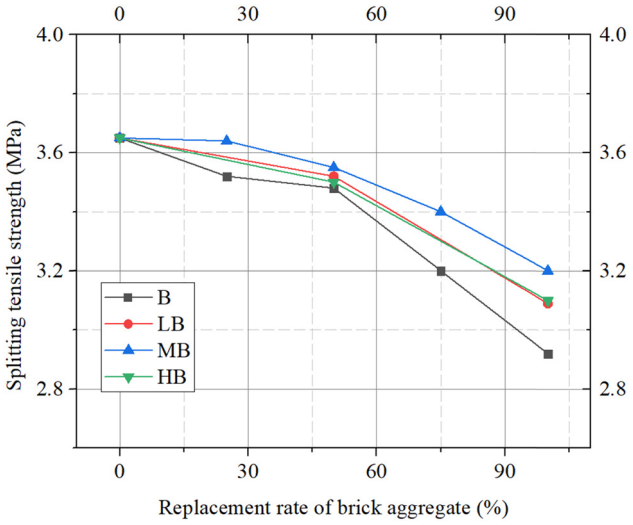

Figure 10: Splitting tensile strength before and after nano-SiO_2 modification.

3.3 Freeze–thaw test phenomenon

The apparent phenomena of each group of concrete specimens after different freeze–thaw cycles are shown in Figure 11. Before the freeze–thaw cycles, the surface of the specimen was smooth, and there was no significant difference between each group of specimens. After 10 freeze–thaw cycles, a small amount of cement mortar fell off the surface of each group of specimens, and there were small holes. The shedding phenomenon of the specimens was not significant, and the apparent phenomenon of each group of specimens was not significantly different. After 20 freeze–thaw cycles, the number of small holes in the P-group specimens increased, and the coarse aggregate was exposed. The surface of the B50-group specimens became rough, there were dense small holes, and the amount of mortar shedding increased. The surface holes in B50-group specimens were smaller than those in MB50-group specimens. As the number of freeze–thaw cycles continued to increase, the aggregate exposure of the P-group specimens was more significant than that of the B50-group and MB50-group, and the number of holes in the B50-group was less than that in the MB50-group. The reasons for this situation are as follows: According to hydrostatic pressure theory [47] and osmotic pressure theory [48], when the freeze–thaw cycle occurs, the large pores in the connected pores will absorb the water in the small pore, thus squeezing the pore wall and causing internal damage to the concrete. For ordinary aggregate concrete, the interface transition zone is equivalent to the large pore, which is the part where freeze–thaw damage occurs. After the interface transition zone is damaged, the aggregate is peeled off from the cement mortar, resulting in the exposure of coarse aggregate. For recycled brick aggregate concrete, due to the large water absorption of recycled brick aggregate, the water in the interfacial transition zone will enter the recycled brick aggregate during the freeze–thaw cycles, which alleviates the pressure in the interfacial transition zone. In addition, the surface of the recycled brick aggregate is rougher, and the pores and cracks are increasingly larger so that the cement slurry flows into the brick aggregate and melts into one. The bonding effect between the recycled brick aggregate and cement mortar is better, which improves the frost resistance of concrete to a certain extent. For nano-SiO_2-modified recycled brick aggregate concrete, nano-SiO_2 fills the cracks and pores on the surface of

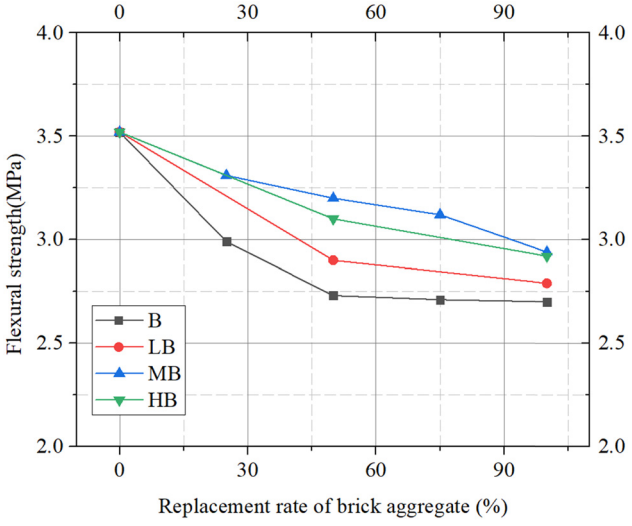

Figure 9: Flexural strength before and after nano-SiO_2 modification.

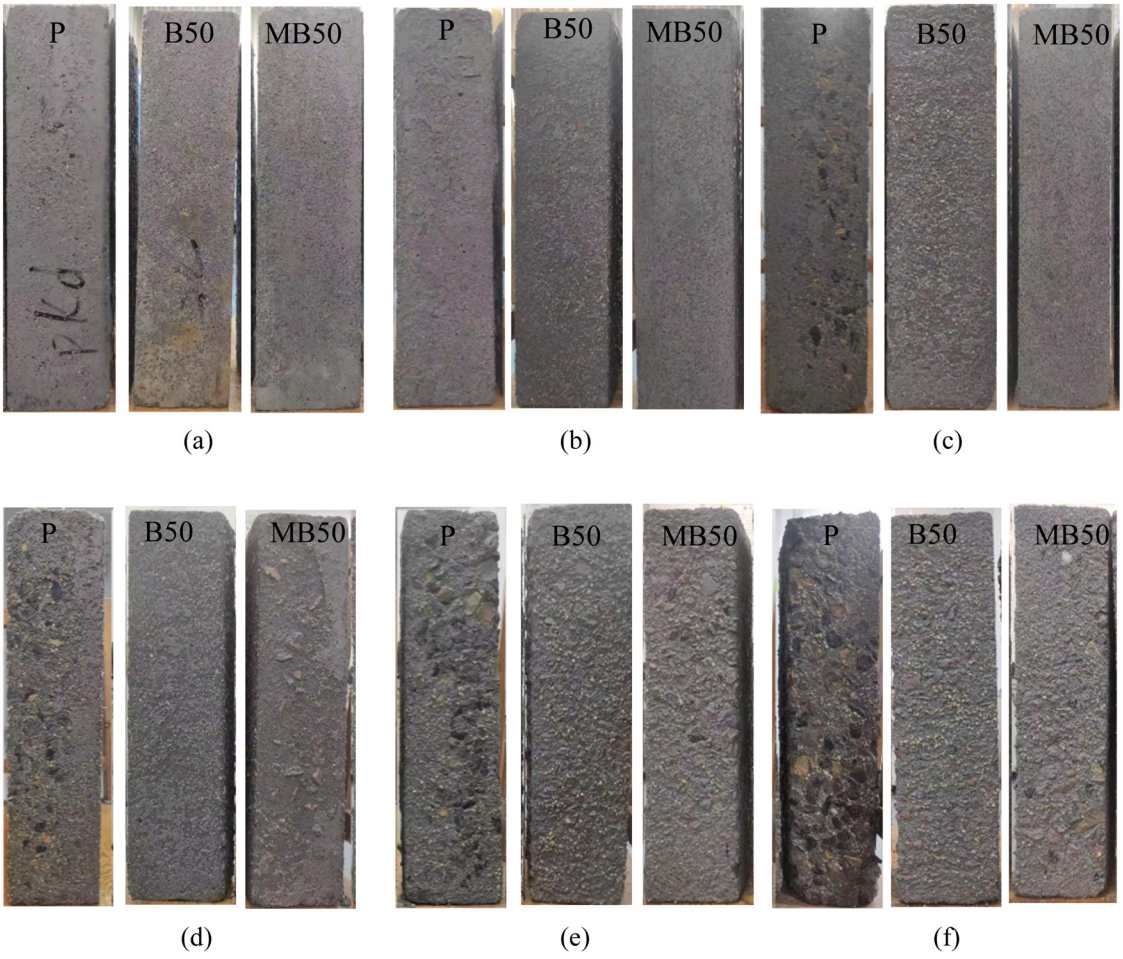

Figure 11: Apparent phenomena of concrete after freeze–thaw cycles. (a) 10 freeze–thaw cycles, (b) 20 freeze–thaw cycles, (c) 30 freeze–thaw cycles, (d) 40 freeze–thaw cycles, (e) 50 freeze–thaw cycles, and (f) 60 freeze–thaw cycles.

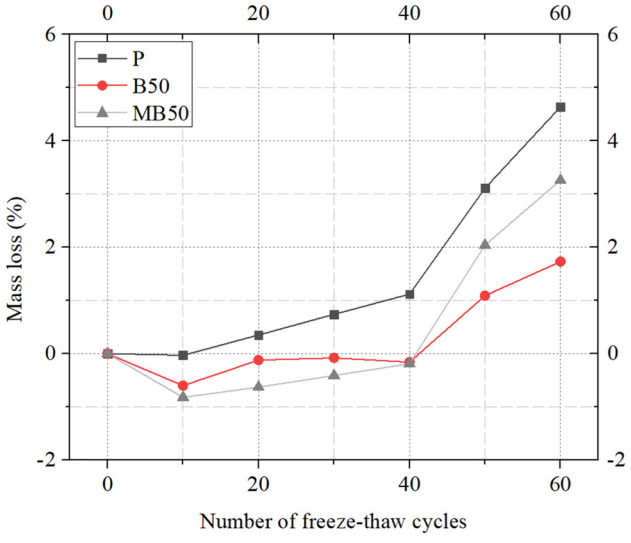

Figure 12: Mass loss of concrete after freeze–thaw cycles.

the recycled brick aggregate, reduces its surface roughness, blocks the passage of cement mortar into the brick aggregate, making it easier for the cement mortar to fall off, and reduces the frost resistance of the concrete.

3.4 Mass loss after freeze–thaw cycles

The mass loss of each group of concrete specimens after different freeze–thaw cycles is shown in Figure 12. Figure 12 shows that as the number of freeze–thaw cycles increased, the mass loss first decreased and then increased. When the number of freeze–thaw cycles was less, the mass loss of the specimen decreased. The reason is that the mass loss of concrete caused by freeze–thaw is less at this time, while the small holes and cracks in the concrete increase after the freeze–thaw cycle, resulting in a larger mass of water absorbed inside the concrete.

In addition, the mass loss of ordinary aggregate concrete was larger than that of recycled brick aggregate concrete. The reason is that the porosity and water absorption of brick aggregate are larger than those of ordinary aggregate, which leads to more water absorption of recycled brick aggregate concrete during freeze–thaw cycles. In addition, recycled brick aggregate has a stronger bonding ability with cement mortar, resulting in less cement mortar shedding.

Before 40 freeze–thaw cycles, the mass loss of recycled brick aggregate concrete was larger than that of nano-SiO_2-modified recycled brick aggregate concrete. After 40 freeze–thaw cycles, the mass loss of recycled brick aggregate concrete was lower than that of nano-SiO_2-modified recycled brick aggregate concrete. This may be because nano-SiO_2 blocks some of the pores in the brick aggregate during the initial stage of freezing and thawing, forming closed pores and resulting in a relatively small frost pressure. As the number of freeze–thaw cycles increases, the pores blocked by nano-SiO_2 gradually connect with the large pores, absorbing a large amount of water and resulting in an increase in frost pressure.

3.5 Relative dynamic elastic modulus after freeze–thaw cycles

The relative dynamic elastic modulus of each group of concrete specimens after different freeze–thaw cycles is shown in Figure 13. The relative dynamic elastic modulus of the concrete specimens presented a downward trend with increasing freeze–thaw cycles. This is due to the increasing freeze–thaw damage of concrete, which leads to a decrease in the relative dynamic elastic modulus. After 60 freeze–thaw cycles, the relative dynamic elastic modulus of ordinary aggregate concrete, recycled brick aggregate concrete, and nano-SiO_2-modified recycled brick aggregate concrete were 52, 60, and 55%, respectively. The appropriate addition of brick aggregate can play the role of an air-entraining agent, thereby enhancing the frost resistance of concrete. However, the nano-SiO_2-modified recycled brick aggregate will prevent the water in the interfacial transition zone from flowing into the brick aggregate, which reduces the effect of the brick aggregate air-entraining agent.

3.6 Compressive strength after freeze–thaw cycles

The compressive strength of each group of concrete specimens after different freeze–thaw cycles is shown in Figure 14. With the increase in the number of freeze–thaw cycles, the compressive strength of concrete decreased gradually. At 15 freeze–thaw cycles, the compressive strength loss of ordinary aggregate concrete and nano-SiO_2-modified recycled brick aggregate concrete was small (compressive strength loss rates were 10 and 16.9%, respectively), while the compressive strength loss of recycled brick aggregate concrete was large (compressive strength loss rate was 26.5%). This is because when the number of freeze–thaw cycles is small, the density of concrete plays a major role in frost resistance. The effective

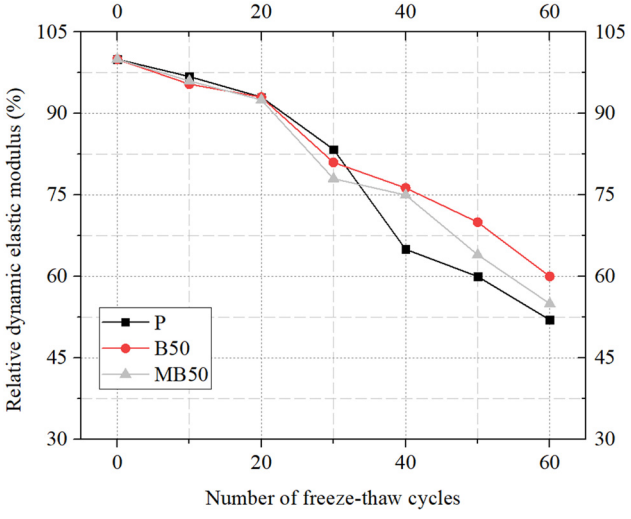

Figure 13: Relative dynamic elastic modulus of concrete after freeze–thaw cycles.

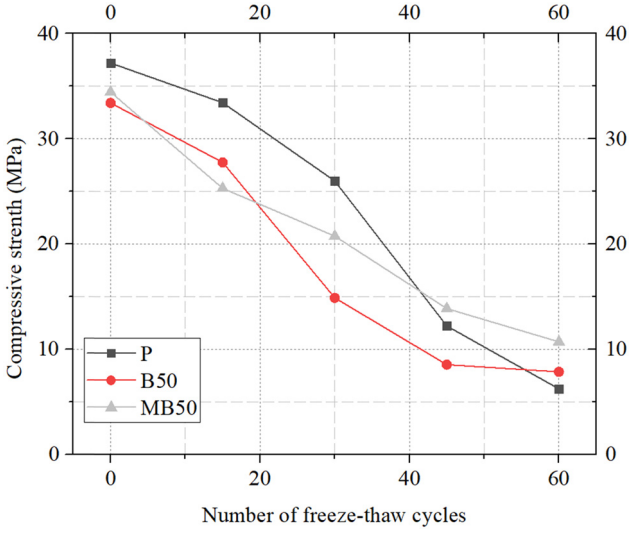

Figure 14: Compressive strength of concrete after freeze–thaw cycles.

water-cement ratio of ordinary concrete is low, and its compactness is larger than that of recycled brick aggregate concrete. Nano-SiO_2 can promote the hydration reaction, so the compactness of nano-SiO_2-modified recycled brick aggregate concrete is also larger than that of recycled brick aggregate concrete.

When the number of freeze–thaw cycles exceeded 15, the compressive strength loss of the concrete began to increase. This is because due to the increase in the number of freeze–thaw cycles, the cement stone on the surface of the specimen continues to fall off, and the free water of the smaller pores gradually produces ice crystals. The specimen is subjected to the expansion of a large number of ice crystals, which gradually accelerates the growth of the compressive strength loss of the specimen. In addition, the compressive strength loss of ordinary aggregate concrete and nano-SiO_2-modified recycled brick aggregate concrete was gradually higher than that of recycled brick aggregate concrete. After 60 freeze–thaw cycles, the compressive strength losses of ordinary aggregate concrete, nano-SiO_2-modified recycled brick aggregate concrete, and recycled brick aggregate concrete were 83.2, 76.4, and 68.9%, respectively. This is because when the number of freeze–thaw cycles is large, the frost damage of concrete is mainly caused by the spalling of cement paste. When the recycled brick aggregate concrete is subjected to freeze–thaw damage, the voids on the surface of the recycled brick aggregate can alleviate the volume expansion pressure caused by water icing, thereby improving its frost resistance; in addition, the surface of the brick aggregate is rough, and the bond strength with the cement paste is stronger, so that the cement paste of the specimen does not easily fall off, which slows down the continuous damage caused by the new pores of the specimen [16]. After nano-SiO_2 modification of the recycled brick aggregate, cracks and holes on the surface of the brick aggregate are filled. When the freezing pressure is too large, nano-SiO_2 hinders the flow of water from the interface transition zone to the brick aggregate, which makes the pressure in the interface transition zone too large, making it easier for the cement stone to fall off the aggregate and reducing the frost resistance of the specimen.

3.7 Microstructure after freeze–thaw cycles

The microstructure of each group of concrete specimens after different freeze–thaw cycles is shown in Figure 15. After freeze–thaw cycles, the cement stone in the interface transition zone of each group of concrete specimens gradually became dispersed, some cement stone was missing, and cracks appeared in the bonding zone with the aggregate. This is due to the action of hydrostatic pressure and osmotic pressure, and cement stone produces cracks and holes, which continue to develop, resulting in cement stone splitting and missing.

Figure 15(a-1, b-1, d-1, e-1) shows that under the same number of freeze–thaw cycles, the interfacial transition zone between stone aggregate and mortar was more likely to produce cracks and pores. The cracks divided the cement mortar into small pieces (a-1), and the separation speed of stone aggregate and cement mortar was faster than that of brick aggregate and cement mortar.

Figure 15(a-2, b-2, d-2, e-2) shows that under the same number of freeze–thaw cycles, the pores in the interfacial transition zone of ordinary aggregate concrete were larger, and the spalling of cement mortar was more serious. Although there were also pores in the interfacial transition zone of recycled brick aggregate concrete, the integrity of the cement stone was good, and there was no large amount of cement stone spalling. This is because the surface of the recycled brick aggregate is rough and the cement mortar can enter the brick aggregate through the pores, so the bonding ability of the recycled brick aggregate and the cement mortar is stronger, and it is not easy to damage after the freeze–thaw cycles. In addition, the pores on the surface of the recycled brick aggregate can alleviate the volume expansion pressure caused by water icing.

Figure 15(c-1, e-1, g-1, h-1) shows that under the same number of freeze–thaw cycles, there were no significant cracks and pores in the cement paste in the interface transition zone of recycled brick aggregate concrete and nano-SiO_2-modified brick aggregate concrete. However, after 45 freeze–thaw cycles, the interfacial transition zone of recycled brick aggregate concrete and nano-SiO_2-modified brick aggregate concrete appeared to have a significant boundary.

Figure 15(d-2, h-2) shows that after 45 freeze–thaw cycles, the cracks and pores of cement mortar in the interfacial transition zone of nano-SiO_2-modified brick aggregate concrete were significantly more than those of recycled brick aggregate concrete. This is due to nano-SiO_2 filling the pores and cracks on the surface of the recycled brick aggregate and reducing its roughness [49], resulting in a decrease in the amount of cement mortar entering the recycled brick aggregate and a decrease in the bond force between the cement mortar and recycled brick aggregate. In addition, nano-SiO_2 hinders the passage of recycled brick aggregates that alleviate water pressure in the interface transition zone.

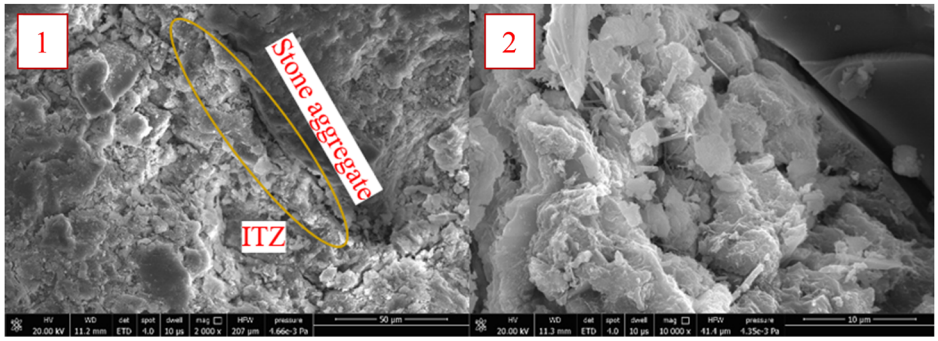

(a)

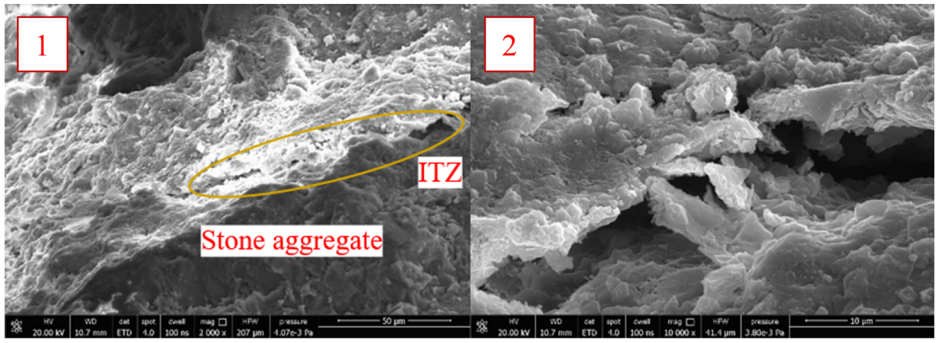

(b)

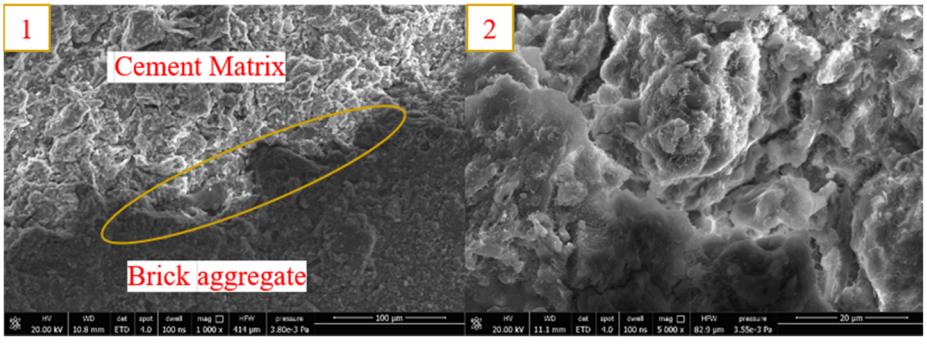

(c)

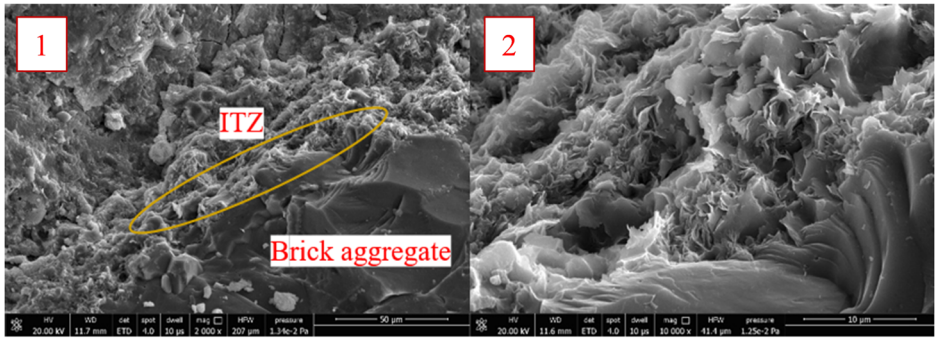

(d)

Figure 15: Microstructure of concrete after freeze–thaw cycles. (a) P after 15 freeze–thaw cycles, (b) P after 45 freeze–thaw cycles, (c) B50 before freeze–thaw cycles, (d) B50 after 15 freeze–thaw cycles, (e) B50 after 45 freeze–thaw cycles, (f) MB50 before freeze–thaw cycles, (g) MB50 after 15 freeze–thaw cycles, (h) MB50 after 45 freeze–thaw cycles, and (i) MB50 after 60 freeze–thaw cycles.

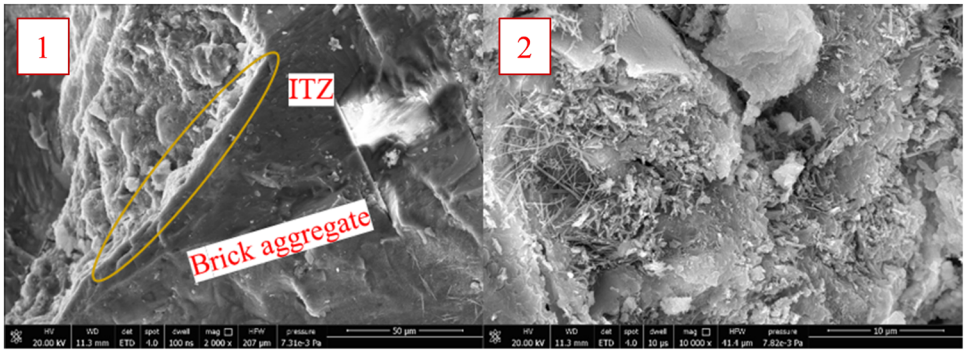

(e)

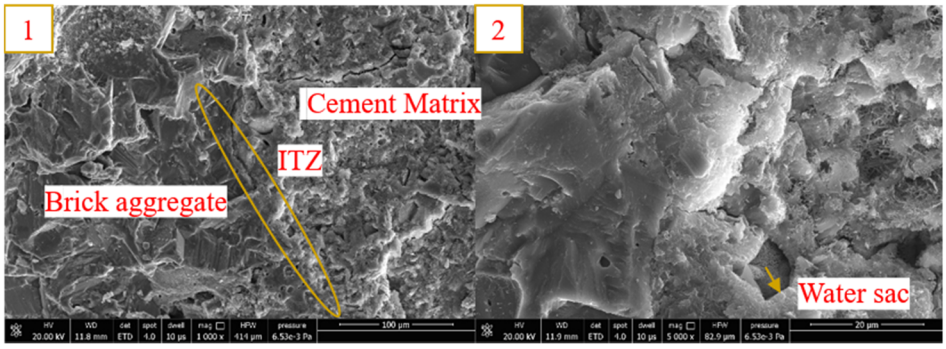

(f)

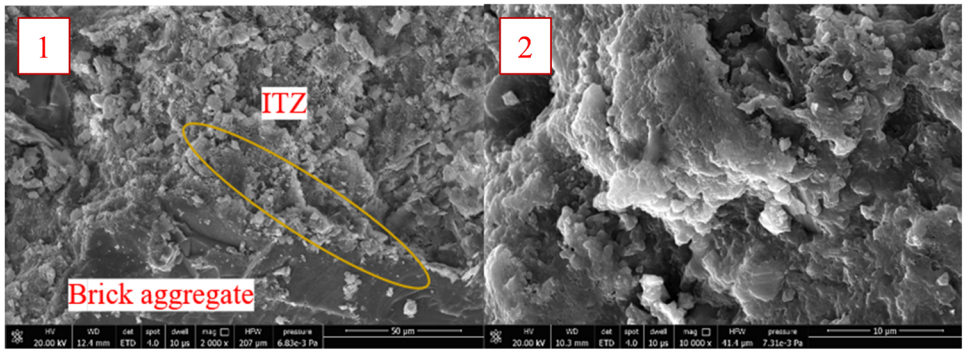

(g)

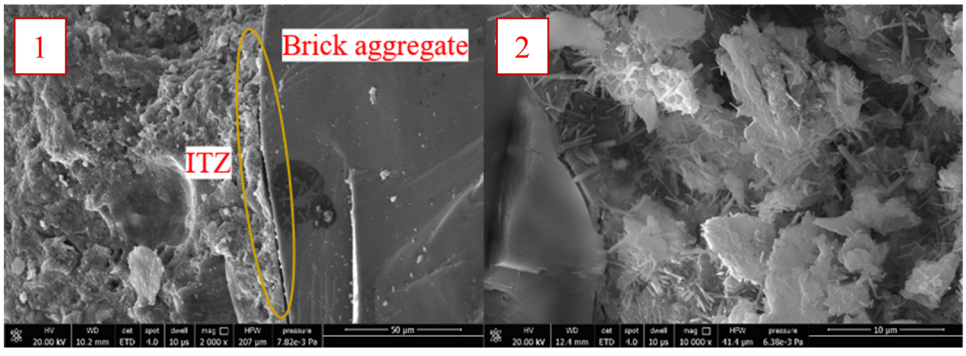

(h)

Figure 15: (*Continued*)

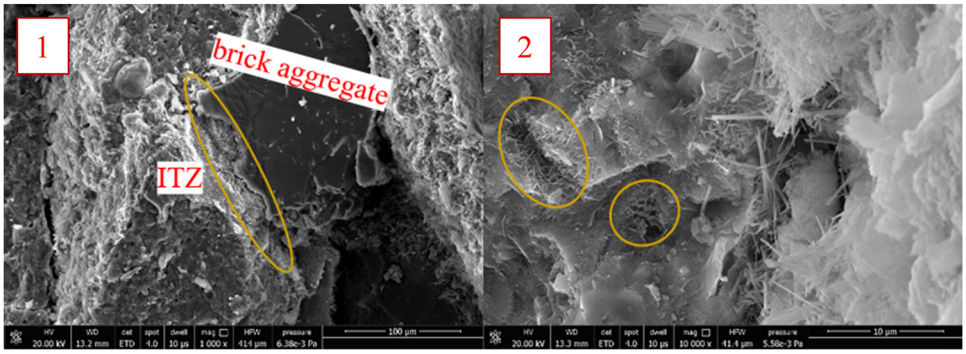

(i)

Figure 15: (*Continued*)

3.8 Freeze–thaw damage mechanism

The concrete freeze–thaw damage schematic diagram is shown in Figure 16. After the concrete was soaked in water for 4 days, water and air sacs coexisted in the pores of the concrete, as shown in Figure 16(a). Ordinary concrete had fewer overall air sacs, ordinary recycled brick aggregate concrete had more air sacs, and nano-modified recycled brick aggregate had the most air sacs. This is because the water cannot completely exclude the air sac in the concrete under normal pressure, and the larger the porosity of the aggregate, the higher the content of the air sacs. The stone aggregate is nearly solid, and there are very few air sacs in ordinary concrete. Brick aggregate has more air sacs due to its high porosity and complexity of pore structure. Although nano-modified concrete reduces the porosity of the transition zone due to the filling of brick aggregates with nanomaterials and the promotion of hydration products in the interface transition zone, it also blocks the channel of water flow into the brick aggregate, resulting in more air sacs in the concrete. This can be proven by the mass loss of concrete during freeze–thaw cycles; that is, when the number of freeze–thaw cycles is small, the concrete mass continues to increase. The degree of mass increase is ordinary concrete < recycled brick aggregate concrete < nano-modified recycled brick aggregate concrete, which reflects the volume of air sacs contained in the concrete.

When the concrete was frozen, the water around the specimen froze from the outside to the inside due to the temperature transfer process, causing the surface water of the specimen to first freeze and form a closed space to wrap the specimen, preventing the flow of water inside and outside the specimen. Then, the water inside the specimen partially froze, resulting in an increase in the volume and movement of the internal water, as shown in Figure 16(b). For ordinary stone aggregate concrete, due to the larger pore size of the interface transition zone than that of cement stone, water flow converged toward the interface transition zone during the freezing process, and the interface transition zone first froze. Due to the lack of air sacs in the interface transition zone to relieve pressure, it is subjected to significant water pressure, resulting in severe freeze–thaw damage. For recycled brick aggregate concrete, due to the smaller pore size of the interface transition zone compared to the internal pores of the brick aggregate, water flowed into the brick aggregate during the freezing process. The water inside the capillary opening carried some air sacs to flow toward the large or small pores; the water inside the small pores carried some air sacs to flow toward the large pores, which could effectively alleviate water pressure. According to osmotic pressure theory, the large pores and small pores in the brick produced greater water pressure, but there were air sacs in the large pores and small pores to relieve the water pressure. Therefore, the degree of damage caused by pore water pressure inside the brick aggregate was limited, and the water pressure in the interface transition zone was very low because brick aggregate absorbed water in the interface transition zone. For nano-modified recycled brick aggregate concrete, the surface pores of the brick aggregate were blocked by nanomaterials and their hydration products, which hindered the flow of water between the interface transition zone and the brick aggregate. The interface transition zone first froze, and then the water flow of small holes in the surrounding cement stone converged toward the interface transition zone. Similar to recycled brick aggregate concrete, the presence of air sacs alleviated water pressure. The water pressure in the interfacial transition zone of nano-modified recycled brick aggregate concrete was larger than that of recycled brick aggregate concrete; the water pressure in the interfacial transition zone of nano-modified recycled brick aggregate concrete was lower than that of ordinary concrete. Therefore, the frost

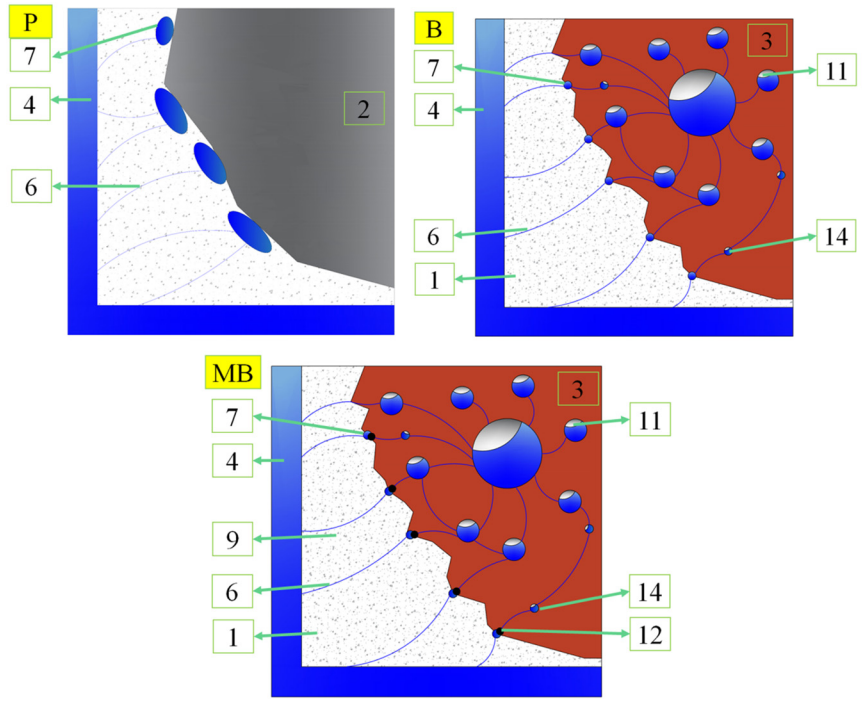

(a)

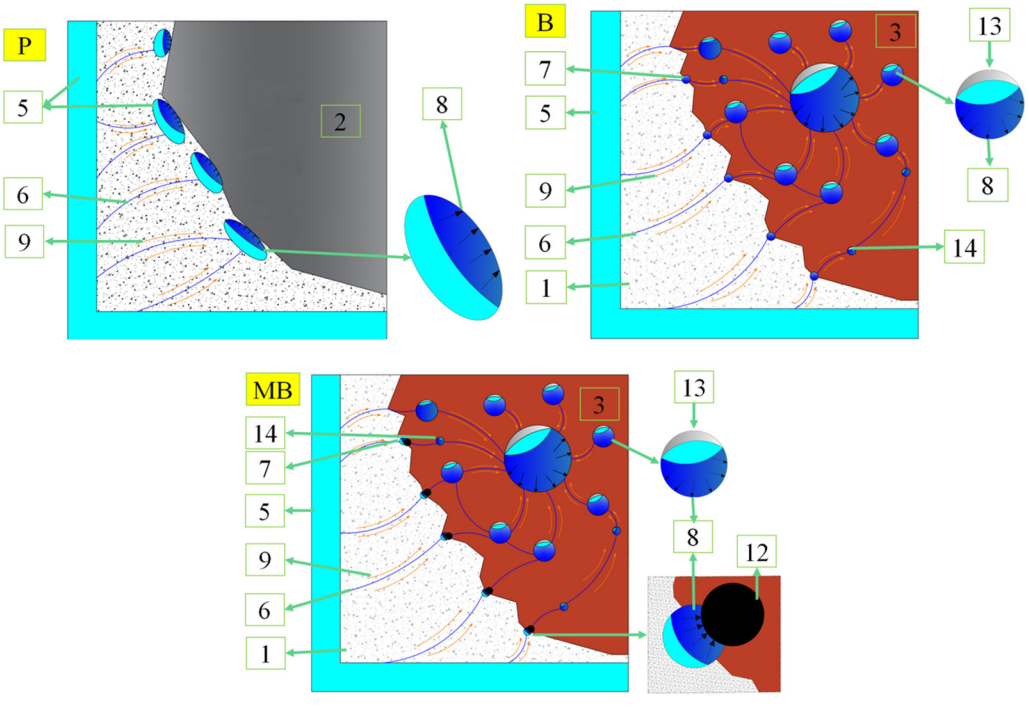

(b)

Figure 16: Concrete freeze–thaw damage schematic diagram. (a) Concrete soaking for 4 days, (b) concrete freezing process, and (c) concrete thawing process.

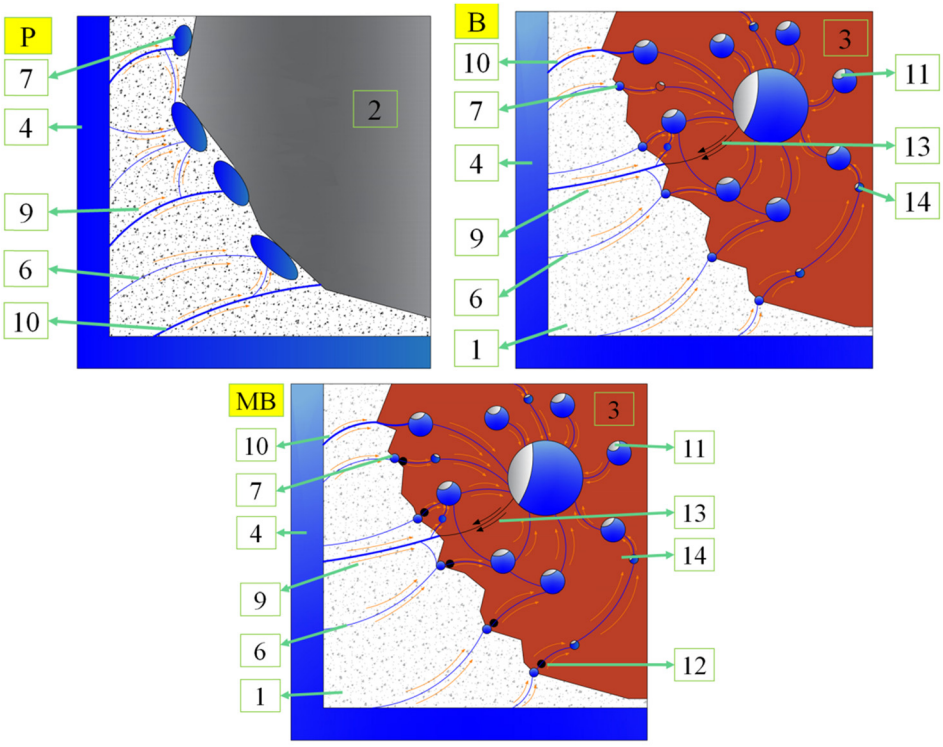

(c)

1 Concrete rock
2 Stone aggregate
3 Recycled brick aggregate
4 Water
5 Ice
6 Water channel in concrete
7 Interface transition zone hole
8 Water pressure in the hole
9 Direction of flowing water
10 Water channel formed by cement stone falling off
11 Air sac
12 Nano-materials and hydration products
13 Air sac outflow external channel
14 Capillary opening

Figure 16: (*Continued*)

resistance of nano-modified recycled brick aggregate concrete was superior to that of ordinary concrete but inferior to that of recycled brick aggregate concrete.

During the thawing process, the external water of the concrete first thawed, and the enclosed space formed by the ice layer disappeared. The internal and external water could flow, as shown in Figure 16(c). Due to the shedding of cement stone during the freeze–thaw process, the concrete formed a deep-water channel inside the specimen (the size of the water channel in ordinary concrete specimens > the size of the water channel in nano-modified recycled brick aggregate concrete > the size of the water channel in recycled brick aggregate concrete). The water channel made the external water enter the interior of the specimen and increased the channel for the air sacs to discharge the specimen, thereby increasing the saturation of the specimen. For ordinary concrete, due to the smooth surface of the stone aggregate, the cement stone was prone to separation and detachment from the stones, which could easily form a water flow channel entering the interior of the specimen, which was detrimental to the frost resistance of the specimen. For recycled brick aggregate concrete, the water pressure in the interfacial transition zone was slowed down, which reduced the speed of cement stone shedding on the surface, thus slowing down the speed of external cracks penetrating into the interior, reducing the growth rate of saturation, and thereby improving the frost resistance of concrete. Compared with recycled brick

aggregate concrete, the water pressure in the interfacial transition zone of nano-modified recycled brick aggregate concrete was higher, and the cement stone fell off relatively faster, which improved the speed of external cracks penetrating into the interior, increasing the growth rate of saturation and thereby reducing the frost resistance of concrete.

3.9 Prediction of frost resistance life

In this study, the damage degree D_n is defined as follows:

$$D_n = \frac{E_0 - E_n}{E_0}, \tag{1}$$

where E_0 is the dynamic elastic modulus without a freeze–thaw cycle; and E_n is the dynamic elastic modulus after n freeze–thaw cycles.

The probability density function of the concrete freeze–thaw cycle life N was established using a two-parameter model as follows [50]:

$$f(N) = \frac{b}{a}\left(\frac{n}{a}\right)^{(b-1)} \exp\left[-\left(\frac{n}{a}\right)^b\right], \tag{2}$$

where a is the scale standard, and b is the shape standard.

The probability distribution function for the life of concrete structures is as follows:

Table 6: Weibull distribution value

	Freeze–thaw cycles	1/$R(n)$	X = ln(n)	Y = ln(ln (1/$R(n)$))
P	10	1.033058	2.302585	−3.425802
	20	1.075269	2.995732	−2.623194
	30	1.199041	3.401197	−1.706379
	40	1.538462	3.688879	−0.842151
	50	1.666667	3.912023	−0.671727
	60	1.923077	4.094345	−0.424760
B50	10	1.048218	2.302585	−3.055660
	20	1.075269	2.995732	−2.623194
	30	1.234568	3.401197	−1.557220
	40	1.310616	3.688879	−1.307493
	50	1.428571	3.912023	−1.030930
	60	1.666667	4.094345	−0.671727
MB50	10	1.041667	2.302585	−3.198534
	20	1.081081	2.995732	−2.551540
	30	1.282051	3.401197	−1.392468
	40	1.333333	3.688879	−1.245899
	50	1.562500	3.912023	−0.806793
	60	1.818182	4.094345	−0.514437

Table 7: Weibull fitting parameters

	b	C	R^2
P	1.78883	−7.69613	0.97472
B50	1.38057	−6.40043	0.95773
MB50	1.54921	−6.88425	0.96955

$$F(N) = 1 - \exp\left[-\left(\frac{n}{a}\right)^b\right]. \tag{3}$$

When subjected to n_1 freeze–thaw cycles, the failure probability of concrete is as follows:

$$P_f(n_1) = 1 - \exp\left[-\left(\frac{n_1}{a}\right)^b\right]. \tag{4}$$

The reliability function can be obtained from the Weibull distribution function as follows:

$$R(n) = 1 - F(n) = \exp\left[-\left(\frac{n}{a}\right)^b\right] = 1 - D(n). \tag{5}$$

Perform a Weibull transformation on equation (5):

$$\ln\left(\ln\left(\frac{1}{Rn}\right)\right) = b(\ln(n) - \ln(a)). \tag{6}$$

Order $Y = \ln(1/R(n))$, $X = \ln(n)$, $C = -b\ln(a)$, and equation (6) could be converted to $Y = Y(X) = bx + C$.

Using the actual number of freeze–thaw cycles as an independent variable, data fitting was performed using Origin software to obtain the Weibull distribution value of the concrete life, as shown in Table 6. Linear fitting

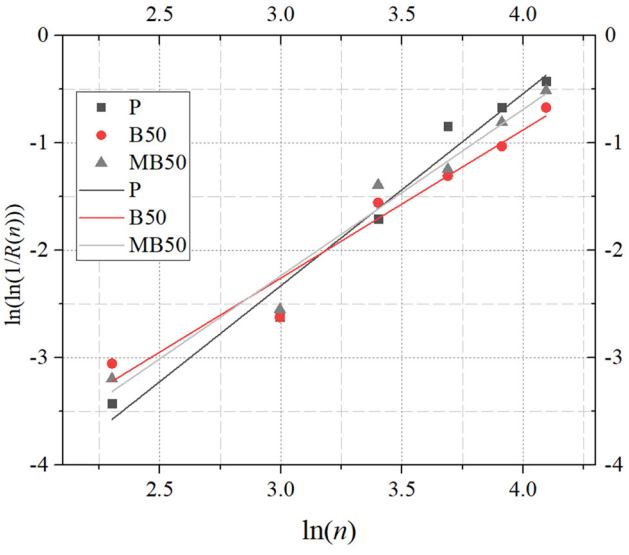

Figure 17: Weibull fitting line.

is performed on the Weibull values in Table 6 to obtain the corresponding Weibull parameter values b and C, as shown in Table 7 and Figure 17.

From Table 7 and Figure 17, it can be seen that the correlation coefficient R^2 was larger than 0.95, indicating that the linear correlation between Y and X was good, that is, the measured data met the Weibull distribution. The Weibull distribution life prediction model for concrete under actual freeze–thaw cycles is as follows:

$$\text{P:}Y = \ln(\ln(1/R(n))) = 1.78883\ln(n) - 7.69613, \quad (7)$$

$$\text{B50}: Y = \ln(\ln(1/R(n))) = 1.38057\ln(n) - 6.40043, \quad (8)$$

$$\text{WB50}: Y = \ln(\ln(1/R(n))) = 1.54921\ln(n) - 6.88425, \quad (9)$$

When $R(n) = 0.6$, the concrete could be judged as invalid. By substituting $R(n) = 0.6$ in the model obtained above, it could be concluded that the ultimate freeze–thaw cycles for ordinary concrete, recycled brick aggregate concrete, and nano-SiO_2-modified recycled brick aggregate concrete were 50, 63, and 55 times, respectively.

4 Conclusion

1) The crushing index and water absorption of nano-SiO_2-modified recycled brick aggregate were lower than those of recycled brick aggregate, and with increasing nano-SiO_2 concentration, the water absorption and crushing index decreased more significantly.
2) After nano-SiO_2 modification, the compressive strength, flexural strength, and splitting tensile strength of recycled brick aggregate concrete were significantly improved. With the increase in the nano-SiO_2 solution concentration, the compressive strength, flexural strength, and splitting tensile strength of recycled brick aggregate concrete first increased and then decreased.
3) With the increase in the number of freeze–thaw cycles, the mortar on the concrete surface fell off and the coarse aggregate was exposed, and the mass loss first decreased and then increased, while the relative dynamic elastic modulus and compressive strength decreased gradually.
4) The frost resistance of recycled brick aggregate concrete was superior to that of ordinary aggregate concrete, while the frost resistance of nano-SiO_2-modified recycled brick aggregate concrete was inferior to that of recycled brick aggregate concrete.
5) The freeze–thaw damage mechanism of recycled brick aggregate concrete was analyzed, and a freeze–thaw damage life prediction model of nano-SiO_2-modified recycled brick aggregate concrete based on the Weibull distribution was proposed.

Funding information: The study was carried out with the support of the Foundation of China Postdoctoral Science Foundation (2022M723687); Doctoral Science and Technology Startup Foundation of Shandong University of Technology (420048); Shandong Province Natural Science Foundation (ZR2021QE209); and Shandong University of Technology Student Innovation and Entrepreneurship Training Program.

Author contributions: Tian Su: investigation, experimental program, funding acquisition, writing – original draft preparation, and review and editing; Shenao Cui: experimental study, data analysis, and writing – original draft preparation; Ting Wang: data analysis, writing – review and editing, and checking the original draft; Zhaochuan Zhang and Xiao Sun: experimental study; Zhenyu Tan and Xuefeng Mei: checking the original draft. All authors have accepted responsibility for the entire content of this manuscript and approved its submission.

Conflict of interest: The authors state no conflict of interest.

Data availability statement: All data generated or analyzed during this study are included in this published article.

References

[1] Su T, Huang ZF, Yuan JF, Zou ZH, Wang CG, Yi HH. Bond properties of deformed rebar in frost-damaged recycled coarse aggregate concrete under repeated loadings. J Mater Civil Eng. 2022;34(10):04022257.
[2] Steve WM, Faiz UAS. Durability properties of high volume fly ash concrete containing nano-silica. Mater Struct. 2015;48:2431–45.
[3] Li HX, Dong LL, Jiang ZW, Yang XJ, Yang ZH. Study on utilization of red brick waste powder in the production of cement-based red decorative plaster for walls. J Clean Prod. 2016;133:1017–26.
[4] Yu Y, Li B, Zhang Y, Zhang C. Deterioration characteristics of recycled aggregate concrete subjected to coupling effect with salt and frost. Rev Adv Mater Sci. 2022;61:27–40.
[5] Viviana L, Ester T, Giacomo M. Mechanical properties of concretes with recycled aggregate and waste brick powder as cement replacement. Procedia Eng. 2017;171:627–32.
[6] Liu X, Wu J, Zhao X, Yan PP, Wu J. Effect of brick waste content on mechanical properties of mixed recycled concrete. Constr Build Mater. 2021;292:123320.
[7] Qiu WL, Teng F, Pan SS. Damage constitutive model of concrete under repeated load after seawater freeze-thaw cycles. Constr Build Mater. 2020;236:117560.

[8] Su T, Wang T, Wang CG, Yi HH. The influence of salt-frost cycles on the bond behavior distribution between rebar and recycled coarse aggregate concrete. J Build Eng. 2022;45:103568.
[9] Yang HF, Liu CL, Jiang JS. Damage constitutive model of stirrup-confined recycled aggregate concrete after freezing and thawing cycles. Constr Build Mater. 2020;253:119100.
[10] Su T, Wu J, Yang GC, Jing XH, Mueller A. Shear behavior of recycled coarse aggregate concrete beams after freezing and thawing cycles. ACI Struct J. 2019;116(5):67–76.
[11] Liu EM, Lin MQ, Xie Q. Research progress on frost resistance property of recycled coarse aggregate concrete. Bull Chin Ceram Soc. 2022;41(9):2963–78 (in Chinese).
[12] Su T, Wang CX, Cao FB, Zou ZH, Wang CG, Wang J, et al. An overview of bond behavior of recycled coarse aggregate concrete with steel bar. Rev Adv Mater Sci. 2021;6(1):127–44.
[13] Feng CH, Cui BW, Guo H, Zhang WY, Zhu JP. Study on the effect of reinforced recycled aggregates on the performance of recycled concrete-synergistic effect of cement slurry-carbonation. J Build Eng. 2023;64(105700):1–16.
[14] Wang JG, Zhang JX, Cao DD, Dang HX, Ding B. Comparison of recycled aggregate treatment methods on the performance for recycled concrete. Constr Build Mater. 2020;234(117366):1–13.
[15] Deng XH, Gao XY, Wang R, Gao MX, Yan XX, Cao WP, et al. Investigation of microstructural damage in air-entrained recycled concrete under a freeze-thaw environment. Constr Build Mater. 2020;268(1):121219.
[16] Wang CX, Zhang D, Cao FB, Wu YH, Ye C, Li L. Research on mechanical properties and damage of recycled concrete after being subjected to freeze-thaw cycles. Ind Constr. 2022;52(05):199–207 (in Chinese).
[17] Zou CY, Fan YH, Hu Q. Experimental study on the basic mechanical property of recycled concrete after freeze-thaw. J Build Mater. 2010;40(S1):434–8 (in Chinese).
[18] Liu J, Hong LIY, Liu DD, Y. Study on the mechanical properties and frost resistance of recycled concrete prepared by village construction wastes. Adv Mater. 2012;418:406–10.
[19] Ji WY. Study on bond behavior between rebar and waste fiber recycled concrete under freeze-thaw conditions. Nanjing Univ Aeronaut Astronaut. 2020 (in Chinese).
[20] Janković K, Bojović D, Nikolić D, Lončar L, Romakov Z. Frost resistance of concrete with crushed brick as aggregate. FU Arch Civ Eng. 2010;8(2):167–8.
[21] Liu KH, Yan JC, Hu Q, Sun Y, Zou CY. Effects of parent concrete and mixing method on the resistance to freezing and thawing of air-entrained recycled aggregate concrete. Constr Build Mater. 2016;106(3):264–73.
[22] Zhu HB, Li X. Experiment on freezing and thawing durability characteristics of recycled aggregate concrete. Key Eng Mater. 2009;400–402(10):447–52.
[23] Richardson A, Coventry K, Bacon J. Freeze/thaw durability of concrete with recycled demolition aggregate compared to virgin aggregate concrete. J Clean Prod. 2011;19(2–3):272–7.
[24] Chen DY, Liu LB, Yan Y, Tan KF, Liu H. Effect of different factors on frost resistance of recycled aggregate concrete. J Wuhan Univ Technol. 2011;13(5):54–8 (in Chinese).
[25] Gokce A, Nagataki S, Saeki T, Hisada M. Freezing and thawing resistance of air-entrained concrete incorporating recycled coarse aggregate: The role of air content in demolished concrete. Cem Concr Res. 2004;34(5):799–806.
[26] Wang XR. Experimental study on the effect of air entrainment on mechanical properties and frost resistance of recycled concrete. Harbin: Harbin Institute of Technology; 2011 (in Chinese).
[27] Meng T, Zhang JL, Wei HD, Shen JJ. Effect of nano-strengthening on the properties and microstructure of recycled concrete. Nanotechnol Rev. 2020;9(1):79–92.
[28] Gao GH, Huang WD, Li CH. Improvement of frost resistance for concrete by coating aggregate with Nano-SiO2. J Build Mater. 2021;24(01):45–53 (in Chinese).
[29] Jo BW, Kim CH, Lim JH, Park JB. Characteristics of cement mortar with nano-SiO2 particles. Constr Build Mater. 2007;21(6):1351–5.
[30] Ozyildirim C, Zegetosky C. Exploratory investigation of nanomaterials to improve strength and permeability of concrete. Transp Res Rec. 2010;2142(1):1–8.
[31] Hou XB, Huang D, Wang W. Recent progress on high performance concrete with nano-SiO2 particles. Concrete. 2013;3:5–9 (in Chinese).
[32] Shahbazpanahi S, Tajara MK, Faraj RH, Mosavi A. Studying the C-H crystals and mechanical properties of sustainable concrete containing recycled coarse aggregate with used nano-silica. Crystals. 2021;11(2):122.
[33] Li L, Xuan DX, Chu SH, Lu JX, Poon CS. Efficiency and mechanism of nano-silica pre-spraying treatment in performance enhancement of recycled aggregate concrete. Constr Build Mater. 2021;301(6):124093.
[34] Chen XY, Cheng ZY, Zhan X, Wu QY. Experimental and numerical research on mechanical properties of recycled concrete with nano-SiO_2-rubber powder. Mater Rep. 2021;35(23):23235–40 + 45 (in Chinese).
[35] Norhasri M, Hamidah MS, Fadzil AM. Applications of using nano material in concrete: A review. Constr Build Mater. 2017;133:91–7.
[36] Zhang P, Li QF, Chen YZ, Shi Y, Ling YF. Durability of steel fiber-reinforced concrete containing SiO_2 nano-particles. Mater. 2019;12(13):2184.
[37] Xu YQ, Li SG, Wang J, Wu XP. Study on influence of nano-material on durability and functionality of concrete. Water Resour Hydropower Eng. 2017;48(9):208–15 (in Chinese).
[38] Deng XH, Gao XY, Wang R, Gao MX, Yan XX, Cao WP, et al. Investigation of microstructural damage in air-entrained recycled concrete under a freeze–thaw environment. Constr Build Mater. 2020;268(1):121219.
[39] Deng XH, Gao XY, Wang R, Zhao CJ. Study of frost resistance and pore distribution change of recycled concrete. Mater Rep. 2021;35(16):16028–34 (in Chinese).
[40] Bankar SN, Nalawade SK. Influence of aggregates treatment on properties of recycled aggregate concrete: A review. IJRASET. 2019;7(7):701–5.
[41] Meng T, Zhang J, Wei H. Effect of nano-strengthening on the properties and microstructure of recycled concrete. Nanotechnol Rev. 2020;9(1):79–92.
[42] Wang T, Wang QS, Cui SA, Yi HH, Su T, Tan ZY. Effects of nano-materials reinforced aggregate on mechanical properties and microstructure of recycled brick aggregate concrete. Mater Sci. 2023;29(3):347–55.
[43] Common Portland Cement, GB175-2007.Cement, GB175-2007. China Standardization Administration, China; 2007 (in Chinese).
[44] Specification for Mix Proportion Design of Ordinary Concrete, JGJ 55-2011pecification for Mix Proportion Design of Ordinary Concrete, JGJ 55-2011. China Academy of Building Research, China; 2011 (in Chinese).

[45] Standard for Test Methods of Concrete Physical and Mechanical Properties, GB/T 50081-2019Test Methods of Concrete Physical and Mechanical Properties, GB/T 50081-2019. China Academy of Building Research, China; 2019 (in Chinese).
[46] Standard for Test Method of Long-Term Performance and Durability of Ordinary Concrete, GB/T 50082-2009. China Academy of Building Research, China; 2009 (in Chinese).
[47] Powers TC. A working hypothesis for further studies of frost resistance. ACI Mater J. 1945;16(4):245–72.
[48] Powers TC, Helmuth RA. Theory of volume changes in hardened Portland cement paste during freezing. Highway research board proceedings; 1953. p. 285–97.
[49] Guo J, Gao M, Wang K, Zhang P. Mechanisms and influential variables on the abrasion resistance hydraulic concrete. Nanotechnol Rev. 2022;11(1):2997–3019.
[50] Xu CD, Zhang P, Lian HD, Wang Y, Li Z, Gu FY. Life prediction of concrete buildings in irrigated areas based on Weibull distribution. Bull Chin Ceram Soc. 2020;39(5):1483–90 (in Chinese).